Relativistically exact eikonal equation for optical fibers with application to adiabatically deforming ring interferometers

Joseph Avron* and Oded Kenneth
Department of Physics, Technion, Haifa, 32000, Israel

(Received 6 June 2016; revised manuscript received 27 September 2016; published 19 December 2016)

We derive the relativistically exact eikonal equation for ring interferometers undergoing deformation. For ring interferometers that undergo slow deformation we describe the two leading terms in the adiabatic expansion of the phase shift. The leading term is independent of the refraction index n and is given by a line integral generalizing results going back to Sagnac for nondeforming interferometers to all orders in $\beta = |\mathbf{v}|/c$. In the nonrelativistic limit this term is $O(\beta)$. The next term in the adiabaticity has the form of a double integral, it is of order β^0 and depends on the refractive index n. It accounts for nonreciprocity due to changing circumstances in the fiber. The adiabatic correction is often comparable to the Sagnac term. In particular, this is the case in Fizeau's interferometer. Besides providing a mathematical framework that puts all ring interferometers under a single umbrella, our results strengthen earlier results and generalize them to fibers with chromatic dispersion.

DOI: 10.1103/PhysRevA.94.063838

I. INTRODUCTION AND SUMMARY OF RESULTS

A ring interferometer has a light source with prescribed frequency which produces two counterpropagating waves which interfere after completing a full cycle. An example is the Sagnac interferometer [1] originally devised to measure the velocity of light relative to the ether but today is perhaps best known because of its close relative, the ring laser gyroscope [5], which literally impacted everyday life. Modern fiber-optics ring interferometers have multiple uses as gyroscopes [6], strain sensors [7], temperatures sensor [8], filters, etc. They have been fertile ground for addressing basic physics and technological issues [2,3,9–15] and have been reviewed in, e.g., [16–18].

The study of the wave equation in moving dielectrics is fraught with both conceptual and technical difficulties [19,20]. A simplification occurs in the the short-wavelength, high-frequency limit, which is described by the eikonal equation [21]. The main drawback of the eikonal is that it disregards backscattering. This is sometimes important [22], but more often the eikonal gives an adequate description of the interference in ring interferometers. As far as relativity is concerned, the eikonal equation is, in principle, exact.

We construct the eikonal equation for deformable fiber interferometers of arbitrary shape, Fig. 1, moving at velocities that may be relativistic ($\beta = |\mathbf{v}|/c \approx 1$) while bending and stretching. We then proceed to describe an expansion of the phase shift for adiabatically deforming fibers.

To describe our results we need to introduce some notation. A thin ring fiber is naturally modeled by a one-dimensional closed curve $\mathbf{x}(t,\theta) \in \mathbb{R}^3$ where the points $\theta = \pm\pi$ are identified. It is convenient to choose a parametrization where θ labels the material points of the fiber.[1] The comoving light source and detector are located at $\theta = \pm\pi$. t is the laboratory time coordinates.

The differential

$$d\mathbf{x} = \mathbf{v}\, dt + \mathbf{e}\, d\theta \tag{1}$$

gives $\mathbf{v}(t,\theta)$, the velocity of the point θ in the laboratory, and $\mathbf{e}(t,\theta)$ the tangent to the curve. The length of the segment $d\theta$ in the laboratory is

$$d\ell = |\mathbf{e}|\, d\theta\,. \tag{2}$$

The eikonal is a nonlinear first-order partial differential equation (PDE) that governs the evolution of the phase of the wave $\phi(t,\theta)$:

$$\pm\frac{\partial\phi}{\partial\theta} = K_\pm(t,\theta,\omega), \quad \omega = -\frac{\partial\phi}{\partial t}. \tag{3}$$

The $\pm$ sign distinguishes the two counterpropagating waves: The $(+)$ wave propagates with θ increasing from $-\pi$ to π and the $(-)$ wave propagates with θ decreasing from π to $-\pi$. The explicit form of $K_\pm$, given in Eq. (29) below, need not concern us at this point.

The phases $d\phi_\pm$, accumulated by the counterpropagating waves as they traverse the interval $d\theta$ are, in general, different. The phase difference $\delta\phi = d\phi_+ - d\phi_- \neq 0$ is known as "nonreciprocity." It has two origins: First, $K_+ \neq K_-$ due to the dependence on the wave propagation direction and moreover, since the two waves visit the interval $d\theta$ at different times $t_+(\theta) \neq t_-(\theta)$, the value of physical parameters making up $K_\pm(t,\theta)$ may have changed.

The amplitude of the wave is governed by suitable transport equations [23] and is slowly varying when the frequency is high. We shall not study it here. Assuming that the amplitudes of the $(\pm)$ waves are the same, the detector output at the time of detection t is proportional to

$$|e^{i\phi_+(t,\pi)} + e^{i\phi_-(t,-\pi)}|^2 = 2\{1 + \cos[\Delta\phi(t)]\},$$
$$\Delta\phi(t) = \phi_+(t,\pi) - \phi_-(t,-\pi). \tag{4}$$

Our goal is to derive an expansion for the phase shift $\Delta\phi(t)$ for fibers that deform adiabatically

Before describing the adiabatic expansion we need to describe the notion of adiabaticity. The $\pm$ waves visit the interval $d\theta$ at different times, $t_\pm(\theta)$. Consequently, the phase difference $\delta\phi = d\phi_+ - d\phi_-$ may depend on the time lapse $\delta t = t_+(\theta) - t_-(\theta)$. For example, the interval $d\theta$ may stretch so that the length $d\ell = |\mathbf{e}|\, d\theta$ seen by the two waves is different. Similarly the refraction index $n(\theta,t,\omega)$ or β may

*avron@physics.technion.ac.il

[1] For a general parametrization see the Appendix.

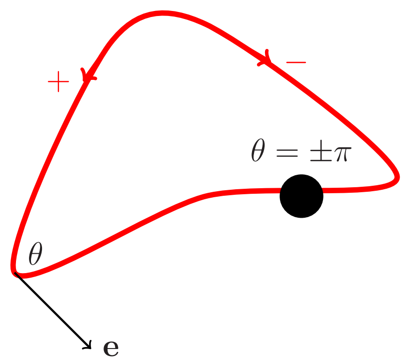

FIG. 1. Ring interferometer represented by a parametrized curve $\mathbf{x}(\theta,t)$ which is a closed loop in space. θ designates a fixed material point on the fiber. $\mathbf{e}(\theta,t)$ is the tangent at a point θ. The two counterpropagating beams are marked with the red arrows and the $\pm$ signs. The black dot represents the comoving light source and detector both located at $\theta = \pm\pi$.

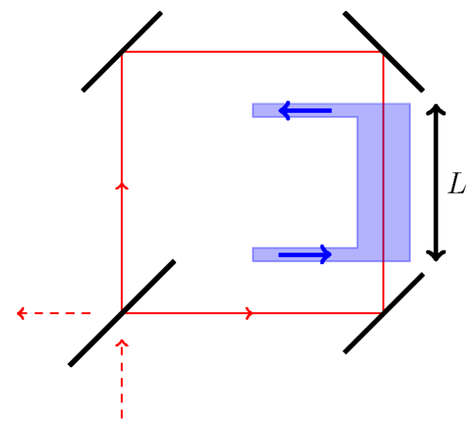

FIG. 2. Schematic of Fizeau interferometer. The three mirrors and beam splitter are at rest in the laboratory. The two counterpropagating beams are denoted by the red arrows. Fluid, say water, is flowing in one arm of the interferometer so one beam is moving with the flow and the other against it.

change between the two visits. We say that the motion of the fiber is adiabatic if all such changes, for all values θ, are small. This is the case if $K_\pm$ changes little in the time τ it takes light to complete a cycle. A natural dimensionless measure of adiabaticity is then

$$\varepsilon = \tau\,\partial_t \ln(K_\pm). \tag{5}$$

If n is time independent and $\beta \ll 1$ then $\tau\partial_t \ln(K_\pm) \approx n\sigma|\mathbf{e}|$ where σ is the rate of stretching of the fiber, see Eq. (14). The adiabatic regime is $|\varepsilon| \ll 1$. For large interferometers and for interferometers with a large number of coils, τ need not be small compared with the time scale of the deformation, and the assumption of adiabaticity may fail.

Our main result is an expansion of the phase shift in powers of ε

$$\Delta\phi = (\Delta\phi)^{(0)} + (\Delta\phi)^{(1)} + \cdots, \tag{6}$$

where $(\Delta\phi)^{(j)} = O(\varepsilon^j)$. The leading term, $(\Delta\phi)^{(0)}(t)$, is given by a line integral at the time of detection t:

$$\begin{aligned}(\Delta\phi)^{(0)} &= -\frac{2\omega_0}{c^2}\int_{-\pi}^{\pi} \gamma^2(\theta)\,\mathbf{v}(\theta)\cdot\mathbf{e}(\theta)\,d\theta \\ &= -\frac{2\omega_0}{c^2}\int_0^L \gamma^2(\ell)\,\mathbf{v}(\ell)\cdot d\boldsymbol{\ell},\end{aligned} \tag{7}$$

where for the sake of typographical simplicity, we have omitted the common argument t everywhere. The length variable ℓ is related to θ by $\ell = \int_{-\pi}^{\theta} |\mathbf{e}(\theta')|\,d\theta'$. $\gamma = (1-\beta^2)^{-1/2}$ and L is the total length of the fiber (at time t). Remarkably, $(\Delta\phi)^{(0)}$ is independent of the (constitutive) dispersion relation n *to all orders in* β. ω_0 is the frequency of the source measured by the laboratory clocks.

In the approximation $\gamma \approx 1$, which is always the case in practice, one recovers the result of [3]. If, in addition, the interferometer moves as a rigid body, the application of the Stokes formula recovers the standard Sagnac area law [2,16,17].

The first-order correction in adiabaticity, $(\Delta\phi)^{(1)}(t)$, has the form of a double integral along the fiber evaluated at the time of detection t. In the nonrelativistic limit we find for $(\Delta\phi)^{(1)}(t)$

$$\begin{aligned}(\Delta\phi)^{(1)} = \frac{\omega}{c^2}\int_{-\pi}^{\pi}\int_{-\pi}^{\pi} &|\mathbf{e}(\theta)|d\theta\,|\mathbf{e}(\theta')|d\theta'\,\partial_\omega[\omega n(\theta')]\,[\partial_t n(\theta) \\ &+ n(\theta)\sigma(\theta)]\ \mathrm{sgn}(\theta'-\theta).\end{aligned} \tag{8}$$

We suppressed the common argument t on both sides. $\sigma = \partial_t \ln|\mathbf{e}(\theta,t)|$ is the (nonrelativistic) stretch rate of the fiber, see Eq. (14) below. Note that while Eq. (7) is independent of n, Eq. (8) depends quadratically on n.

Note that $(\Delta\phi)^{(0)} = O(\beta\varepsilon^0)$, while $(\Delta\phi)^{(1)} = O(\varepsilon\beta^0)$. In principle, ε and β are independent parameters.[2] When $\varepsilon \ll \beta$, $(\Delta\phi)^{(1)}$ is a small correction to $(\Delta\phi)^{(0)}$ and in the opposite case $\varepsilon \gg \beta$, $(\Delta\phi)^{(0)}$ is a small correction to $(\Delta\phi)^{(1)}$. When $\varepsilon \sim \beta$ the two terms are comparable. This is the case in Fizeau's interferometer [24], shown schematically in Fig. 2. Although this is not a fiber interferometer, the theory still applies and as we shall show in Sec. VI B von Laue's classical formula [25] for the phase shift in Fizeau is simply the sum of the two terms

$$\frac{2\omega}{c^2} V L\,[n\partial_\omega(\omega n) - 1] = (\Delta\phi)^{(0)} + (\Delta\phi)^{(1)}, \tag{9}$$

where V is the velocity of the flow and L the length of the pipe [3,10].

II. SPACE-TIME GEOMETRY OF A MOVING RING

A moving curve in Minkowski space-time can be described by a vector valued function of two variables: $\mathbf{x}(t,\theta) \in \mathbb{R}^3$. There is freedom in choosing parametrization for the curve. A convenient parametrization is to choose t to be the laboratory time coordinate and θ labeling the material points of the fiber. The velocity and tangent to the curve are given in Eq. (1). It follows that

$$\partial_t \mathbf{e} = \partial_\theta \mathbf{v}. \tag{10}$$

[2] If the length scale of the deformations is comparable to the length of the fiber and the velocities associated with them are comparable to the rigid body part of the velocity, then $\varepsilon \sim \beta$.

The (laboratory frame) line element is $d\boldsymbol{\ell} = \mathbf{e}\, d\theta$. Since $\mathbf{v}$ is a velocity of a material point on the fiber, $\mathbf{v}\cdot\mathbf{v} < 1$ in units where $c = 1$ which we henceforth use.

If $\mathbf{e}$ is parallel to $\mathbf{v}$, the proper length[3] of the segment $d\ell'$ is related to the length $d\ell$ by Lorentz contraction, $\gamma\, d\ell = d\ell'$. If, however, $\mathbf{e}\cdot\mathbf{v} = 0$ there is no contraction and $d\ell = d\ell'$. In general, $d\ell$ and $d\ell'$ are related by

$$\frac{d\ell}{\gamma_\perp} = \frac{d\ell'}{\gamma}, \quad \gamma = \frac{1}{\sqrt{1-\mathbf{v}^2}}, \quad \gamma_\perp = \frac{1}{\sqrt{1-(\mathbf{v}\times\hat{\mathbf{e}})^2}}. \tag{11}$$

This can be seen from

$$\begin{aligned}(d\ell')^2 &= (d\ell'_\perp)^2 + (d\ell'_\parallel)^2 = (d\ell_\perp)^2 + \frac{(d\ell_\parallel)^2}{1-\mathbf{v}^2}\\ &= \gamma^2[(d\ell)^2 - \mathbf{v}^2(d\ell_\perp)^2]\\ &= \gamma^2 (d\ell)^2\big(1-\mathbf{v}_\perp^2\big) = \left(\frac{\gamma\, d\ell}{\gamma_\perp}\right)^2.\end{aligned} \tag{12}$$

The fibers are allowed to stretch. The stretch rate σ is naturally defined as the rate of change of proper length, measured in proper time (as measured by an observer comoving with the point θ of the fiber):

$$\sigma = \gamma\,\partial_t \ln\frac{d\ell'}{d\theta}, \quad \frac{d\ell'}{d\theta} = \frac{\gamma}{\gamma_\perp}|\mathbf{e}|. \tag{13}$$

To leading order in β

$$\sigma \approx \partial_t \ln|\mathbf{e}| = \frac{\mathbf{e}\cdot\dot{\mathbf{e}}}{\mathbf{e}\cdot\mathbf{e}} = \frac{\mathbf{e}\cdot\partial_\theta\mathbf{v}}{\mathbf{e}\cdot\mathbf{e}}. \tag{14}$$

No stretching means $\sigma = 0$.

The world line of a fixed material point θ is

$$X(t,\theta) = (t,\mathbf{x}(t,\theta)) \in \mathbb{R}^4, \quad -\infty < t < \infty, \tag{15}$$

The union of the world lines for all θ gives a two-dimensional tube shown in Fig. 3.

$$\mathcal{M} = \big\{X = (t,\mathbf{x}(t,\theta))\big|, \quad \theta\in[0,2\pi], \quad t\in\mathbb{R}\big\}. \tag{16}$$

The tangent vectors to $\mathcal{M}$ are spanned by $T' = \partial_t X = (1,\mathbf{v})$ and $E = \partial_\theta X = (0,\mathbf{e})$. The scalar product is induced from the embedding four-dimensional Minkowski space:

$$\begin{aligned}T'\cdot T' &= \partial_t X\cdot\partial_t X = 1 - \mathbf{v}\cdot\mathbf{v},\\ E\cdot E &= \partial_\theta X\cdot\partial_\theta X = -\mathbf{e}\cdot\mathbf{e},\\ T'\cdot E &= \partial_\theta X\cdot\partial_t X = -\mathbf{e}\cdot\mathbf{v},\end{aligned} \tag{17}$$

The metric on $\mathcal{M}$, in the coordinates (θ,t), is given by

$$dX\cdot dX = (1-\mathbf{v}^2)(dt)^2 - 2\,\mathbf{e}\cdot\mathbf{v}\,dt\,d\theta - \mathbf{e}^2\,(d\theta)^2. \tag{18}$$

Note that the coordinates are not Lorentz orthogonal.

$E = \partial_\theta X$ is the direction of simultaneity in the laboratory. We shall denote by $\hat{E}$ the normalized version of E. The time direction in a comoving frame is given by $T' = \partial_t X$. Its normalized version $\widehat{T}' = \gamma T'$ corresponds to the four-velocity of the material point with fixed θ. Explicitly

$$\widehat{T}' = \gamma\,\partial_t X = \gamma(1,\mathbf{v}), \quad \widehat{E} = \frac{\partial_\theta X}{|\mathbf{e}|} = (0,\hat{\mathbf{e}}), \tag{19}$$

[3] As measured by an observer comoving with the material point of the fiber labeled as θ.

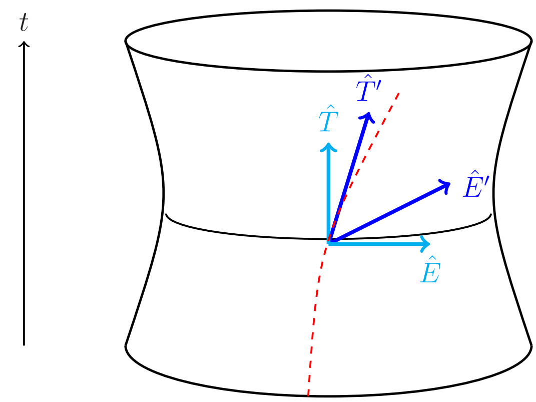

FIG. 3. Two-dimensional world tube $\mathcal{M}$ associated with a moving closed curve in Minkowski space-time. The red curve is the world line of a fixed material point of the fiber labeled by θ in the text. The Lorentz orthonormal frame $(\hat{T},\hat{E})$ distinguishes the time and space axis in the laboratory. Similarly, $(\hat{T}',\hat{E}')$ distinguishes the time and space axis in the comoving frame attached to θ.

The spatial direction of the comoving Lorentz frame is the tangent vector E' which is Minkowski orthogonal to T':

$$E' = E - (E\cdot\widehat{T}')\widehat{T}' = \partial_\theta X + \gamma^2\mathbf{v}\cdot\mathbf{e}\,\partial_t X. \tag{20}$$

The Minkowski length of E' is

$$\begin{aligned}E'\cdot E' &= E\cdot E - (E\cdot\widehat{T}')^2 = -\mathbf{e}^2 - \gamma^2(\mathbf{e}\cdot\mathbf{v})^2\\ &= -\gamma^2[\mathbf{e}^2 - (\mathbf{v}\times\mathbf{e})^2] = -\frac{\gamma^2}{\gamma_\perp^2}\mathbf{e}^2 = -\left(\frac{d\ell'}{d\theta}\right)^2.\end{aligned} \tag{21}$$

For the sake of completeness we note that the tangent vector to $\mathcal{M}$ associated with the laboratory time is

$$T = T' - (\widehat{E}\cdot T')\widehat{E} = (1,0). \tag{22}$$

$(\widehat{T},\widehat{E})$ and $(\widehat{T}',\widehat{E}')$ are Lorentz orthogonal frames related by standard Lorentz transformation. In contrast, the frame $(\widehat{T}',\widehat{E})$ associated with the coordinates (t,θ) is not Lorentz orthogonal and so is not related to $(\widehat{T}',\widehat{E}')$ by the standard Lorentz transformation.

III. EIKONAL

In a local comoving frame the wave vector k' and frequency ω' are related by the dispersion relation[4]

$$k' = \pm n(t,\theta,\omega')\omega'. \tag{23}$$

These local inertial frames do not provide a global frame on $\mathcal{M}$ because clocks associated with different local frames at different θ cannot be synchronized. We need to translate Eq. (23) to a relation between $\partial_t\phi$ and $\partial_\theta\phi$.

By definition,

$$\omega' = -\nabla_{\widehat{T}'}\phi, \quad k' = \nabla_{\widehat{E}'}\phi. \tag{24}$$

Using Eq. (19) we thus have

$$\omega' = -\gamma\,\partial_t\phi = \gamma\omega, \tag{25}$$

[4] Allowing t dependence of n implicitly also allows it to depend on the curvature of the fiber.

and using Eqs. (20) and (21)

$$k' = \frac{d\theta}{d\ell'}(\partial_\theta + \gamma^2 \mathbf{v}\cdot\mathbf{e}\partial_t)\phi. \tag{26}$$

Remark. Because the time derivative $\partial_t = (\partial_t)_\theta$ is taken at constant value of the comoving coordinate θ, it has the physical meaning of a derivative taken with the flow. Had we used the laboratory coordinate (x,t) it would have taken the Eulerian form $\partial_t + \mathbf{v}\cdot\nabla$ and Eq. (25) would have taken the standard form of a Doppler shift. The comoving coordinates (θ,t) are, however, not inertial and hence the transformation takes a different form.

Substituting ω' and k' from Eqs. (25) and (26) in Eq. (23) we find

$$\frac{d\theta}{d\ell'}(\partial_\theta + \gamma^2 \mathbf{v}\cdot\mathbf{e}\,\partial_t)\phi = \mp\gamma\, n\, \partial_t\phi, \quad n = n(t,\theta,\gamma\omega) \tag{27}$$

Rearranging gives the eikonal equation

$$\pm\frac{\partial\phi}{\partial\theta} = K_\pm(t,\theta,\omega), \quad \omega = -\frac{\partial\phi}{\partial t}, \tag{28}$$

where

$$\begin{aligned} K_\pm(t,\theta,\omega,) &= K_1(t,\theta,\omega,) \pm K_2(t,\theta,\omega,) \\ &= \gamma^2\frac{\omega}{c}\left(\frac{n(t,\theta,\gamma\omega)}{\gamma_\perp} \pm \frac{\mathbf{v}\cdot\hat{\mathbf{e}}}{c}\right)|\mathbf{e}|. \end{aligned} \tag{29}$$

We have now reintroduced c. $K_\pm$ is a dimensionless version of the wave number encoding all the relevant information on the fiber and its motion. (See the Appendix, Sec. 3.)

In the nonrelativistic limit where $\gamma,\gamma_\perp \approx 1$,

$$K_\pm \approx \frac{\omega}{c}\left(n \pm \frac{\mathbf{v}\cdot\hat{\mathbf{e}}}{c}\right)|\mathbf{e}|. \tag{30}$$

The eikonal, Eq. (28), is a nonlinear, first-order PDE. In the case that n is nondispersive, it simplifies to a linear PDE. In either case, the PDE can be solved by the method of characteristics, which reduces the problem of solving a PDE to solving a set of coupled ordinary differential equations (ODEs) [26]. We describe this reduction in the next section.

A. Hamiltonian system

The eikonal equation (28) has the form of a Hamilton-Jacobi equation of mechanics. Table I gives the dictionary that translates wave properties to mechanical properties. This allows us to easily write the characteristic equations and reduces solving the PDE for the phase $\phi_\pm(\theta,t)$ to a problem in mechanics.

The phase $\phi_\pm(t,\theta)$ is the analog of the action $S(x,t)$ which can be determined by solving the Hamilton equations for (x,p) and then integrating

$$dS = pdx - Hdt = (p\dot{x} - H)dt = Ldt \tag{31}$$

along the classical path. We shall do precisely the same thing for $\phi_\pm$.

The analog of phase space in the context of the eikonal is the time-frequency plane (t,ω) and the analog of time in mechanics is the coordinate θ of the fiber. Hence, the analog of Hamilton equations are

$$\pm\frac{dt_\pm}{d\theta} = \partial_\omega K_\pm, \quad \pm\frac{d\omega_\pm}{d\theta} = -\partial_t K_\pm. \tag{32}$$

The equation for $\omega_\pm$ may be interpreted as Doppler shifts along the fiber.

The evolution of the phase ϕ along the fiber is now

$$d\phi_\pm = \mp\mathcal{L}_\pm\, d\theta, \tag{33}$$

where $\mathcal{L}_\pm$ is the Legendre transform of $K_\pm$:

$$\begin{aligned} \mathcal{L}_\pm &= \pm\omega\frac{dt_\pm}{d\theta} - K_\pm = \omega\partial_\omega K_\pm - K_\pm \\ &= \omega\partial_\omega K_1 - K_1 = \frac{\omega^2}{c}\gamma\,(\partial_\omega n)\,\frac{d\ell'}{d\theta}. \end{aligned} \tag{34}$$

In the third identity we used the fact that K_2 is linear in ω so its Legendre transform vanishes identically. This shows that $\mathcal{L}_+ = \mathcal{L}_- = \mathcal{L}$. In the absence of dispersion,[5] $\mathcal{L} = 0$. To first order in β

$$\mathcal{L} \approx \frac{\omega^2}{c}(\partial_\omega n)\,|\mathbf{e}|. \tag{35}$$

Once we find the solutions $[t_\pm(\theta),\omega_\pm(\theta)]$ for the Hamiltonian system, the phase $\phi_\pm$ can be obtained by integrating Eq. (33) along the trajectory.

B. Boundary conditions

We now turn to the boundary conditions for the Hamiltonian system, Eqs. (32), governing the flow of the phase-space points $(t_\pm,\omega_\pm)$ and $\phi_\pm$, Eqs. (33) and (34). Consider Fig. 4. We are interested in solutions $t_\pm(\theta)$ that terminate simultaneously at the detector at t_d. This imposes *final* conditions on $t_\pm(\theta)$:

$$t_+(\pi) = t_-(-\pi) = t_d. \tag{36}$$

Note that the emission times are not specified and the $\pm$ waves may have different emission times:

$$t_{e+} = t_+(-\pi), \quad t_{e-} = t_-(\pi). \tag{37}$$

The second boundary condition fixes $\omega_\pm(\theta)$ to be the frequency of the source $\omega_0(t_e)$ at the time of emission:

$$\omega_\pm(\mp\pi) = \omega_0(t_{e\pm}) = \left.\frac{\omega_0'}{\gamma_\pi}\right|_{t=t_{e\pm}}, \quad \gamma_\pi(t) = \gamma(t,\pi), \tag{38}$$

TABLE I. Correspondence between Hamilton-Jacobi equations in mechanics and the eikonal equation.

Mechanics		Eikonal	
Phase space	(x,p)	Time-frequency plane	(t,ω)
Position	x	Time	t
Momentum	p	Frequency	ω
Time	t	Fiber coordinate	$\pm\theta$
Action	$S(x,t)$	(minus) Phase	$-\phi(t,\theta)$
Hamiltonian	$H(x,p,t)$	Dimensionless wave number	$K_\pm(t,\theta,\omega)$
Lagrangian	$L(t,x,v)$	$\mathcal{L}$	$\omega\partial_\omega K - K$

[5]This reflects the fact that in the absence of dispersion, $t_\pm(\theta)$ equals the time schedule of a constant phase along the fiber.

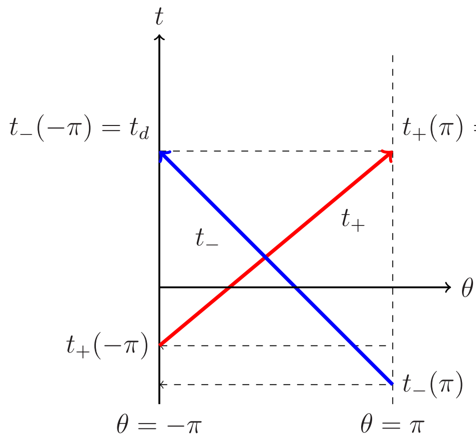

FIG. 4. Characteristics for the $+$ wave (red arrow) and the $-$ wave (blue arrow) in the fiber. Both terminate at the detector simultaneously at laboratory time t_d. The characteristics are parametrized by θ. The interfering waves have different times of emission. This difference is one source for the phase shift. The other source is the evolution of the phase along the characteristics.

where we assumed that the source has a constant frequency ω_0' in its own rest frame. The phase of the source is

$$\Phi = -\omega_0' t' = -\omega_0' \int^t \frac{ds}{\gamma_\pi(s)}, \tag{39}$$

and one may therefore write the boundary condition on $\omega_\pm$ as

$$\omega_\pm(\mp\pi) = -\left(\frac{d\Phi}{dt}\right)(t_{e\pm}). \tag{40}$$

The boundary conditions for the Hamiltonian system (t,ω) are nonstandard: Final boundary conditions are imposed on $t_\pm(\theta)$ while initial boundary conditions are imposed on $\omega_\pm(\theta)$. The mixture of initial and final boundary conditions is unusual from the perspective of mechanics and ODE in general[6]. It is illustrated pictorially in Fig. 5.

Finally, we turn to the boundary conditions for the phase in the interferometer.[7] The phase $\phi_\pm$ of the $\pm$ waves are set at their emission times by the phase of the source. The boundary values for $\phi_\pm$ are then the initial values at the time of emission and are given by

$$\phi_\pm(\mp\pi) = \Phi(t_{e\pm}). \tag{41}$$

It follows by Eq. (33) that the phase at the detector is then given by

$$\phi_\pm(\pm\pi) = \Phi(t_\pm(\mp\pi)) - \int_{-\pi}^{\pi} \mathcal{L}(t_\pm(\theta),\omega_\pm(\theta),\theta)\, d\theta. \tag{42}$$

[6]Mixed boundary conditions also show up in the semiclassical limit of quantum mechanics [27].

[7]In the case of a ring laser gyroscope, the boundary conditions are replaced by resonance conditions on the phase $\phi_\pm$.

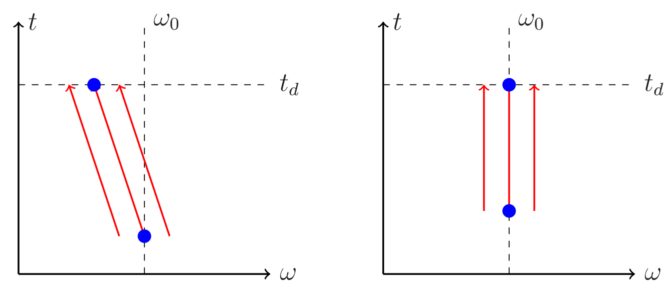

FIG. 5. Hamiltonian vector fields on the time-frequency plane shown as red arrows. t_d is the detection time and ω_0 the frequency of the source at emission time. The boundary conditions at $\theta = \pm\pi$ select the orbit that starts on the vertical line ω_0 and terminates on the horizontal line t_d. This is the orbit that connects the blue dots. The figure on the right shows the situation in the stationary case: ω is conserved as can be seen from the fact that the vector field in phase space is vertical.

The phase difference of the $\pm$ waves at the detector is given by

$$\Delta\phi = \delta\Phi - \int_{-\pi}^{\pi} (\delta\mathcal{L}) d\theta, \tag{43}$$

where

$$\delta\Phi = \Phi(t_{e+}) - \Phi(t_{e-}) = -\omega_0' \int_{t_{e-}}^{t_{e+}} \frac{ds}{\gamma_\pi(s)}, \tag{44}$$

and

$$\delta\mathcal{L} = \mathcal{L}(t_+,\theta,\omega_+) - \mathcal{L}(t_-,\theta,\omega_-). \tag{45}$$

In the framework of geometric optics $\phi_\pm$ are large quantities and $\Delta\phi$, being the difference of two large quantities, should be handled with care. As we see, when the fiber motion is adiabatic and $\beta \ll 1$, the first term in Eq. (43) is an integral over a short time interval and the second has an almost self-canceling integrand.

IV. STATIONARY INTERFEROMETERS

We say that an interferometer is stationary in the comoving coordinates (t,θ) if[8]

$$\omega_0 = \text{const.}, \quad \partial_t K_\pm = 0. \tag{46}$$

This setting corresponds to having only the term of $O(\varepsilon^0)$ in the adiabatic expansion, i.e., to $\Delta^{(0)}$. The condition $\omega_0 = \text{const.}$ expresses the stationarity of the light source. The fiber is stationary in the (t,θ) coordinates if $n,|\mathbf{e}|,\gamma,\gamma_\perp$, and $\mathbf{e}\cdot\mathbf{v}$ are time independent. This gives $\partial_t K = 0$. This holds for a Sagnac interferometer (of arbitrary shape) rotating like a rigid body with constant angular velocity and also for nonstretching treadmill fiber interferometers[9] moving at constant speed, such

[8]A more general notion of stationarity may be defined by demanding the existence of a time like Killing vector field on the world tube. Since our analysis is tied to the comoving coordinates we only consider translation under $(\partial/\partial_t)_\theta$. For a formulation in terms of arbitrary coordinates, see the Appendix.

[9]For planar fibers one may show that these are the only two possibilities of stationary motions.

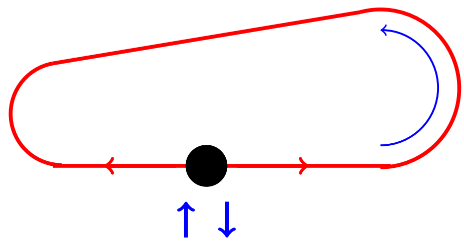

FIG. 6. Example of stationarity. The optical fiber moves like a treadmill in the direction marked by the blue arrow. The black dot represents the comoving beam splitter and the two vertical arrows the light source and detector. The counterpropagating light beams share a common path and are marked by red arrows. If the fiber moves at constant speed without stretching, $\partial_t K_\pm = 0$, and the interferometer is stationary in the sense of Eq. (46).

as the one shown in Fig. 6. Stationarity is a strong condition and few examples satisfy it exactly. However, it is often satisfied approximately. In such cases the stationarity assumption is useful as a basis for the adiabatic approximation described in the next section.

The statement $\partial_t K_\pm = 0$ implies by Eq. (32) that $\omega_\pm(\theta)$ is constant on each trajectory. The boundary conditions on $\omega_\pm$ then say that

$$\omega_+ = \omega_- = \frac{\omega_0'}{\gamma_\pi} = \omega_0. \tag{47}$$

Since the source has constant frequency in the laboratory, $\omega_\pm$ are also constant.

It also follows from $\partial_t K_\pm = 0$ that $\mathcal{L}$ is time independent. Consequently [see Eq. (45)], $\delta\mathcal{L}$ vanishes identically and we are left with

$$\begin{aligned}\Delta\phi &= -\omega_0' \int_{t_{e-}}^{t_{e+}} \frac{ds}{\gamma_\pi(s)} = \frac{\omega_0'}{\gamma_\pi}(t_{e-} - t_{e+}) \\ &= -\omega_0(t_{e+} - t_{e-}) = -\omega_0 \Delta t_e,\end{aligned} \tag{48}$$

where Δt_e is the difference in times of emission and we made use of the fact that the source is in stationary motion. The elapsed times between emission and detection is given by

$$(t_d - t_e)_\pm = t_\pm(\pm\pi) - t_\pm(\mp\pi) = \int_{-\pi}^{\pi} \partial_\omega K_\pm d\theta. \tag{49}$$

Since $K_\pm$ does not depend on t or ϕ and since ω is a constant, the integrand is a known function of θ. Using the fact that the detection times for the $(\pm)$ waves are the same, $t_+(\pi) = t_d = t_-(-\pi)$, the difference in the emission times is given by

$$\begin{aligned}\Delta t_e &= t_+(-\pi) - t_-(\pi) = -\int_{-\pi}^{\pi} (\partial_\omega K_+ - \partial_\omega K_-) d\theta \\ &= -2\int_{-\pi}^{\pi} \partial_\omega K_2\, d\theta \\ &= -2\int_{-\pi}^{\pi} \gamma^2 \mathbf{v}\cdot\mathbf{e}\, d\theta = -2\oint \gamma^2 \mathbf{v}\cdot d\ell.\end{aligned} \tag{50}$$

This completes the proof of Eq. (7).

Geometric optics is concerned with the regime $\omega_0\tau \gg 1$. Since

$$(\Delta\phi)^{(0)} = O[\beta\gamma^2(\omega_0\tau)], \tag{51}$$

the phase shift depends sensitively on the velocity via $\beta\gamma^2$. This is both a bug and a feature. It is a feature in the sense that phase shifts of $O(1)$ allow us to measure the velocity with great accuracy. It can be a bug because small fluctuations of the velocity can make the interference pattern unstable. Ring interferometers become increasingly sensitive and eventually unstable at relativistic velocities. The optimal regime for the ring interferometers is when the velocity is adjusted to the frequency ω_0 so that the phase shift is $O(1)$.

V. ADIABATIC CORRECTION

We say that the interferometer is adiabatic if the Hamiltonian $K_\pm$ and the source frequency ω_0'/γ_π change little during a cycle time $\tau \sim L/c$ of a light pulse through the fiber[10]

$$[\tau\partial_t \ln(K_\pm),\ \tau\partial_t \ln(\gamma_\pi)] \sim \varepsilon \ll 1. \tag{52}$$

We shall now consider the leading adiabatic corrections $\Delta^{(1)}$ which we will find to be of order $O[\varepsilon(\omega_0\tau)] = O[\varepsilon\beta^0(\omega_0\tau)]$. Comparison with Eq. (51) shows that $\Delta^{(1)}$ may be as large as $\Delta^{(0)}$ even for $\varepsilon \ll 1$ provided that $\beta \ll 1$. For this reason and for simplicity we shall assume in the following $\beta \ll 1$. In particular it allows neglecting $K_2 = O(\beta\omega\tau)$ in comparison with $K_1 = O(\omega\tau)$ in Eq. (29).

The adiabatic expansion of (t,ω) can be organized as

$$\begin{aligned}t_\pm(\theta) &= t_d + t_\pm^{(0)}(\theta) + t_\pm^{(1)}(\theta) + \cdots, \\ \omega_\pm(\theta) &= \omega_0 + \omega_\pm^{(1)}(\theta) + \cdots,\end{aligned} \tag{53}$$

where

$$t_\pm^{(0)} = O(\tau), \quad t_\pm^{(1)} = O(\varepsilon\tau), \quad \omega_\pm^{(1)} = O(\varepsilon\omega_0). \tag{54}$$

From Eq. (43)

$$(\Delta\phi)^{(1)} = (\delta\Phi)^{(1)} - \int_{-\pi}^{\pi} (\delta\mathcal{L})^{(1)} d\theta. \tag{55}$$

We have already seen in the previous section [see Eq. (50)] that

$$\Delta t_e^{(0)} = t_+^{(0)}(-\pi) - t_-^{(0)}(\pi) = O(\beta). \tag{56}$$

It follows that at leading order in β we may neglect all powers of $\Delta t_e^{(0)}$ and write

$$(\delta\Phi)^{(1)} \approx -\omega_0 \Delta t_e^{(1)} = -\omega_0[t_+^{(1)}(-\pi) - t_-^{(1)}(\pi)]. \tag{57}$$

Since $\tau\partial_t\mathcal{L}/\mathcal{L} = O(\varepsilon)$ while $\omega_0\partial_\omega\mathcal{L}/\mathcal{L} = O(1)$ we have

$$\delta\mathcal{L}^{(1)} \approx (\partial_t\mathcal{L})\,\delta t^{(0)} + (\partial_\omega\mathcal{L})\,\delta\omega^{(1)}, \tag{58}$$

where $\partial\mathcal{L} = (\partial\mathcal{L})(t_d,\theta,\omega_0)$ are evaluated at the detection time and

$$\begin{aligned}\delta t^{(0)}(\theta) &= t_+^{(0)}(\theta) - t_-^{(0)}(\theta), \\ \delta\omega^{(1)}(\theta) &= \omega_+^{(1)}(\theta) - \omega_-^{(1)}(\theta).\end{aligned} \tag{59}$$

[10]More systematically, the adiabatic limit is represented by writing $K_\pm$ and γ_π as functions of scaled dimensionless time $s = \varepsilon t/\tau$ rather than of t.

To compute $(\Delta\phi)^{(1)}$ we therefore need $t_\pm^{(1)}$ at the emission point and $(\delta t^{(0)},\delta\omega^{(1)})$ along the fiber. Interestingly, as we will see below, we will not need $\omega^{(1)}$.

The dominant piece of $t_\pm^{(0)}$ is of $O(\tau)$ and comes from K_1. A piece of $O(\tau\beta)$ comes from K_2. It is the smaller piece that gives the Sagnac effect at order ε^0. For evaluating Eq. (58) to leading order in β we only need the dominant part of $t_\pm^{(0)}$, which is the solution of

$$\pm\frac{dt^{(0)}}{d\theta}\approx\partial_\omega K_1(t_d,\theta,\omega_0). \tag{60}$$

Hence

$$t_\pm^{(0)}(\theta)\approx\mp\int_\theta^{\pm\pi}\partial_\omega K_1(t_d,\theta',\omega_0)\,d\theta'. \tag{61}$$

This gives

$$\delta t^{(0)}(\theta)\approx\int_{-\pi}^{\pi}\mathrm{sgn}(\theta-\theta')\partial_\omega K_1(t_d,\theta',\omega_0)\,d\theta'. \tag{62}$$

We need $t_\pm^{(0)}$ to find $t_\pm^{(1)}$, which is the solution of

$$\pm\frac{dt^{(1)}}{d\theta}\approx(t^{(0)}\partial_t+\omega^{(1)}\partial_\omega)\partial_\omega K_1(t_d,\theta,\omega_0). \tag{63}$$

Integrating Eq. (63) we find

$$\begin{aligned}(\delta\Phi)^{(1)}&=-\omega_0[t_+^{(1)}(-\pi)-t_-^{(1)}(\pi)]\\&=\omega_0\int_{-\pi}^{\pi}d\theta[\delta t^{(0)}(\theta)\partial_t+\delta\omega^{(1)}(\theta)\partial_\omega]\partial_\omega K_1(t_d,\theta,\omega_0).\end{aligned} \tag{64}$$

$(\Delta\phi)^{(1)}$ has four terms: two that come from the integral in Eq. (64) and two from integrating Eq. (58). Summing these four terms gives

$$\begin{aligned}(\Delta\phi)^{(1)}=\int d\theta\big[&\delta\omega^{(1)}(\theta)\big(\omega\partial_\omega^2K-\partial_\omega\mathcal{L}\big)\\&+\delta t^{(0)}(\theta)(\omega\partial_\omega\partial_tK-\partial_t\mathcal{L})].\end{aligned} \tag{65}$$

The first bracketed subtraction vanishes since

$$\omega\partial_\omega^2K-\partial_\omega\mathcal{L}=\omega\partial_\omega^2K-\partial_\omega(\omega\partial_\omega K)+\partial_\omega K=0. \tag{66}$$

The second subtraction is

$$\omega\partial_\omega\partial_tK-\partial_t\mathcal{L}=\omega\partial_\omega\partial_tK-\partial_t(\omega\partial_\omega K-K)=\partial_tK. \tag{67}$$

The term proportional to $\delta\omega^{(1)}$ drops and the term proportional to $\delta t^{(0)}$ survives. Substituting Eq. (62) and using Eq. (67) gives

$$\begin{aligned}(\Delta\phi)^{(1)}&=\int_{-\pi}^{\pi}\int_{-\pi}^{\pi}d\theta\,d\theta'\,\mathrm{sgn}(\theta-\theta')\partial_tK_1(\theta)\partial_\omega K_1(\theta')\approx\frac{\omega}{c^2}\int_{-\pi}^{\pi}\int_{-\pi}^{\pi}d\theta\,d\theta'\,\mathrm{sgn}(\theta-\theta')\partial_t(n|\mathbf{e}|)(\theta)\partial_\omega(\omega n|\mathbf{e}|)(\theta')\\&\approx\frac{\omega}{c^2}\int_{-\pi}^{\pi}\int_{-\pi}^{\pi}|\mathbf{e}(\theta)|d\theta\,|\mathbf{e}(\theta')|\,d\theta'\,\mathrm{sgn}(\theta-\theta')[\partial_tn(\theta)+n(\theta)\sigma(\theta)]\,\partial_\omega[\omega n(\theta')]\\&=\frac{\omega}{c^2}\int_0^L\int_0^L d\ell\,d\ell'\,\mathrm{sgn}(\ell-\ell')[\partial_tn(\ell)+\partial_t\ell\,\partial_\ell n(\ell)+n(\ell)\sigma(\ell)]\partial_\omega[\omega n(\ell')].\end{aligned} \tag{68}$$

For typographical simplicity we have omitted the arguments t and ω throughout. In the first line we used the $\beta\ll1$ approximation $K_1\approx\frac{\omega}{c}n|\mathbf{e}|$. In the second line we used the nonrelativistic approximation for the stretch rate σ, Eq. (14). In the last line we changed variables from θ to ℓ so that $n(\theta,t)$ is replaced by $n(\ell,t)$. L is the length of the fiber at the time of detection t and $\partial_t\ell=\int_0^\ell\sigma(\ell')d\ell'$. This proves Eq. (8).

VI. APPLICATIONS

A. Thermal nonreciprocity

Consider a static homogeneous fiber with a temperature profile $T(\theta,t)$ whose variation δT is small. The index of refraction is assumed to be a function of the temperature, $n(T,\omega)$, and similarly the length $d\ell$ is a function of T, i.e. $d\ell=|\mathbf{e}(T)|d\theta$. The coefficient of thermal expansion is then $\alpha=\partial_T\ln|\mathbf{e}(T)|$. We are interested in computing $\Delta\phi^{(1)}$ to first order in δT. This problem has been considered in [4].

Evidently

$$\partial_t(n|\mathbf{e}|)=\partial_T(n|\mathbf{e}|)\,\partial_t(\delta T). \tag{69}$$

This implies that the first bracketed factors in Eq. (68), all three lines, is $O(\delta T)$ and we may ignore the δT dependence of the other factors. For a homogeneous fiber the second bracketed factor in line 1 are a constant which can be pulled out of the integral.

$$\begin{aligned}(\Delta\phi)^{(1)}&\approx\frac{\omega}{c^2}\int_{-\pi}^{\pi}\int_{-\pi}^{\pi}d\theta\,d\theta'\,\mathrm{sgn}(\theta-\theta')\partial_t(n|\mathbf{e}|)(\theta)\\&\quad\times\partial_\omega(\omega n|\mathbf{e}|)(\theta')\\&\approx\frac{\omega}{c^2}\partial_T(n|\mathbf{e}|)\partial_\omega(\omega n|\mathbf{e}|)\\&\quad\times\int_{-\pi}^{\pi}\int_{-\pi}^{\pi}d\theta\,d\theta'\,\mathrm{sgn}(\theta-\theta')\partial_t(\delta T)\\&\approx2\frac{\omega}{c^2}|\mathbf{e}|(\partial_Tn+n\alpha)\partial_\omega(\omega n|\mathbf{e}|)\int_{-\pi}^{\pi}d\theta\,\theta\,\partial_t(\delta T).\end{aligned} \tag{70}$$

Changing variables from θ to length $\ell=|\mathbf{e}|(\theta+\pi)$ we can write

$$\begin{aligned}(\Delta\phi)^{(1)}\approx\frac{\omega}{c^2}(\partial_Tn+n\alpha)\partial_\omega(\omega n)\int_0^L d\ell\,(2\ell-L)[\partial_t(\delta T)\\+\partial_t\ell\,\partial_\ell(\delta T)].\end{aligned} \tag{71}$$

However, for static fibers $\partial_t\ell$ vanishes apart from a $\sim\alpha\delta T$ correction which is negligible to leading order in δT. Hence

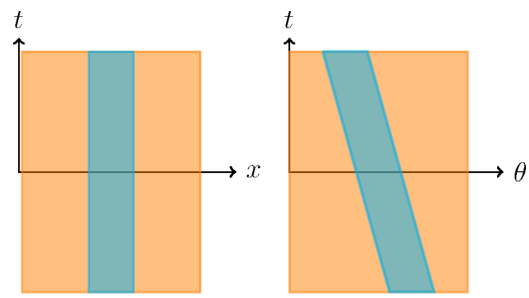

FIG. 7. Velocity in the right arm of the Fizeau interferometer. Shown on the left is the velocity of the fluid as a function of the laboratory coordinates (t,x). The orange strip represents zero velocity and the cyan velocity V. In the laboratory frame the velocity is independent of t and the setting is stationary. The diagram on the right illustrates the velocity field in the (t,θ) coordinates. The velocity is nonzero in the (cyan) parallelogram. We assume that a fluid particle starting at the entrance boundary discontinuously changes its velocity from zero to V, and then stops abruptly at the exit boundary. The velocity is time dependent, reflecting nonstationarity in the (t,θ) coordinates.

to first order in δT

$$(\Delta\phi)^{(1)} \approx \frac{\omega}{c^2}(\partial_T n + n\alpha)\partial_\omega(\omega n)\int_0^L d\ell\,(2\ell - L)[\partial_t(\delta T)]. \tag{72}$$

This is a slight generalization of the Shupe formula [4] in that it accounts also for the case that n is dispersive.

Note that if the spatial distribution of $\partial_t(\delta T)$ has short-range correlations (idealized by white noise) then the expectation of $[(\Delta\phi)^{(1)}]^2$ is

$$\mathbb{E}([(\Delta\phi)^{(1)}]^2) = O(L^3), \tag{73}$$

which, for large L, dominates the Sagnac $O(L)$ term.

B. Fizeau

The Fizeau experiment is shown schematically in Fig. 2. The interferometer is at rest in the laboratory, but one arm of the interferometer has a flowing liquid, say, water. From the perspective of the laboratory the setting is stationary, because the velocity at each point in the laboratory frame is time independent.[11] However, from the point of view of the comoving coordinate θ, the interferometer is not stationary: Elements of the fluid accelerate and decelerate as they enter and leave the pipe. Figure 7 compares the laboratory (x,t) and (θ,t) coordinates.

In the laboratory coordinates the velocity is approximately given by

$$v(x) = V\chi_{(x_{\rm in},x_{\rm out})}(x), \tag{74}$$

where $\chi_{(x_{\rm in},x_{\rm out})}$ is the characteristic function of the interval. The stretching is then

$$\sigma = \partial_t \ln|\mathbf{e}| = \frac{\partial_\theta v}{|\mathbf{e}|} = \partial_x v = V[\delta(x - x_{\rm in}) - \delta(x - x_{\rm out})]. \tag{75}$$

Substituting Eq. (74) into Eq. (7) (and using $|\mathbf{e}|d\theta = dx$) gives for the Sagnac term

$$(\Delta\phi)^{(0)} = -2\omega V L. \tag{76}$$

Substituting Eq. (75) into Eq. (8) gives the correction due to stretching:

$$\begin{aligned}(\Delta\phi)^{(1)} &= n\omega\partial_\omega(\omega n)\int \sigma(x)\,\mathrm{sgn}(x' - x)\,dx\,dx' \\ &= n\omega\partial_\omega(\omega n)2VL.\end{aligned} \tag{77}$$

Summing we obtain the von Laue result, Eq. (9).

ACKNOWLEDGMENT

We are especially grateful to Amos Ori for getting us interested in this problem and for many instructive and insightful discussions. We thank B. Shapiro for telling us about Refs. [19,20], and M. Tur for a useful conversation. Figures 1, 2, and 6 were taken from [3]. The research is supported by Israel Science Foundation. J.E.A. gratefully acknowledges the hospitality of the Simons Center for Geometry and Physics, Stony Brook University, where some of the research for this paper was performed.

APPENDIX: MOVING FIBERS IN ARBITRARY COORDINATES

1. World sheet in general coordinates

A closed optical fiber deforming in time traces out a two-dimensional surface in space-time which, in analogy to string-theorist terminology, may be referred as a "world sheet." One may describe it parametrically as $X = X^\mu(t,s)$, where t is a timelike coordinate and s is a spacelike periodic coordinate (i.e., $\dot{X}^\mu = \partial_t X^\mu$ and $X'^\mu = \partial_s X^\mu$ are timelike and spacelike, respectively). The refraction index of the fiber is $n(t,s,\omega)$.

To fully describe the fiber one must also be given its local four-velocity. This is given by a tangent vector field[12] v on the world sheet. We write it using two components $v = (v^0,v^1)$. The (unit) four-vector corresponding to it is

$$v^i\partial_i X^\mu = v^0\dot{X}^\mu + v^1 X'^\mu. \tag{A1}$$

The three functions $X^\mu(t,s)$, $v^\mu(t,s)$, and $n(t,s,\omega)$ suffice to fully describe our system.

It is convenient to define another tangent vector $e = (e^0,e^1)$ by demanding it to be orthogonal to v and normalized. (Its orientation may be chosen by demanding $e^1 > 0$.) It is possible to write e explicitly in terms of v, the Levi-Civita tensor ε, and the metric $g_{ij} = \eta_{\mu\nu}\partial_i X^\mu \partial_j X^\nu$. The pair (v,e) form a two-dimensional vierbein on the world sheet.

[11] Analysis of the Fizeau interferometer from this point of view is given in the Appendix, Sec. A 5.

[12] The world-sheet tangent vectors v,e defined here should not be confused with the spatial vectors mentioned in the main text.

2. Eikonal equation

Within the eikonal approximation, a wave moving in the fiber is described by its phase $\phi(t,s)$. The corresponding frequency and wave vector are than defined to be

$$\omega = -\partial_t\phi, \quad k = \partial_s\phi. \tag{A2}$$

The standard relation $k' = \pm n\omega'$ is satisfied, however, by the wave vector k' and frequency ω' in the local inertial frame (v,e) moving with the fiber, that is,

$$\omega' = -v^i\partial_i\phi = v^0\omega - v^1 k, \quad k' = e^i\partial_i\phi = -e^0\omega + e^1 k. \tag{A3}$$

In the absence of chromatic dispersion one easily solves $k' = \pm n\omega'$ obtaining

$$k = \omega\frac{e^0 \pm nv^0}{e^1 \pm nv^1}. \tag{A4}$$

When considering dispersive media one must keep in mind that the refraction index n appearing here should be evaluated at the local moving frame, i.e.,

$$n = n(\omega') = n(v^0\omega - v^1 k). \tag{A5}$$

Thus to really find $k(\omega)$ may require solving a nontrivial equation. This difficulty is avoided if one chooses s to be a comoving coordinate (such that each value of s corresponds to a specific fixed material point) since then $v^1 \equiv 0$ and hence $n = n(v^0\omega)$ does not depend on k. Also in the nonrelativistic limit one typically has $v^1 \ll v^0$ (unless the coordinates t,s are chosen in a very unnatural way). Expanding in powers of β then allows a perturbative solution for $k(\omega)$.

The two solutions of Eq. (A4) define two functions of ω,t,s which we shall denote by $\pm K_\pm(t,s,\omega)$. (The extra sign in front of K is needed for consistency with the rest of our conventions. Under nonextreme circumstances it corresponds to having both K_+ and K_- positive.) Having found the functions $K_\pm$, the Hamilton equations for the eikonal wave propagation can be written in the standard form:

$$\pm\frac{dt}{ds} = \partial_\omega K_\pm, \quad \pm\frac{d\omega}{ds} = -\partial_t K_\pm, \tag{A6}$$

$$\frac{d\phi}{ds} = \mp\mathcal{L}_\pm, \quad \mathcal{L}_\pm = \omega\partial_\omega K_\pm - K_\pm. \tag{A7}$$

3. Consistency with Eq. (29)

Choosing $s = \theta$ a comoving coordinate means that the matter particles move in the direction defined by ∂_t and hence $v^1 \equiv 0$. If we further assume that t is the laboratory time such that $X = (t,\mathbf{x}(t,\theta))$, then we may also solve for v^0,e^0,e^1 obtaining

$$v^0 = \gamma, \quad e^1 = \frac{\gamma_\perp}{\gamma|\mathbf{x}'|}, \quad e^0 = \gamma\gamma_\perp\dot{\mathbf{x}}_\parallel. \tag{A8}$$

This reproduces $K_\pm$ of Eq. (29):

$$K_\pm = \frac{\gamma^2}{\gamma_\perp}n\omega|\mathbf{x}'| \pm \gamma^2\omega(\dot{\mathbf{x}}\cdot\mathbf{x}').$$

4. Stationarity

The fiber and the associated interferometer may be called stationary if there exists a timelike vector field ξ defined on the world sheet under which the system is symmetric. This means that the ξ-Lie derivative of v,n,g_{ij} vanish. Note that this is equivalent to vanishing of the ξ-Lie derivative of v,e,n. In Sec. IV we considered only the case of $\xi = v$ (which made the condition $L_\xi v = 0$ trivial). The simplest nontrivial example of a stationary interferometer with $\xi \neq v$ is the Fizeau experiment.

5. Fizeau yet again

The Fizeau experiment is described most simply in terms of the laboratory coordinates (t,x) where it is explicitly time independent. Denoting the fluid velocity by V (which may depend on x but not on t) we have

$$v = (\gamma,\gamma V), \quad e = (\gamma V,\gamma), \tag{A9}$$

with

$$K_\pm = \omega\frac{n(\omega') \pm V}{1 \pm Vn(\omega')}. \tag{A10}$$

Noting that in the nonrelativistic limit

$$\omega' = \gamma(\omega - Vk) = \omega \mp V\omega n(\omega) + O(\beta^2),$$

we obtain

$$K_\pm = n_0\omega \pm \left(1 - n_0^2\right)V\omega \mp V\omega^2 n_0\partial_\omega n_0 + O(\beta^2),$$

where we denoted $n_0 = n(\omega)$ in order to distinguish it from $n(\omega')$.

Since $K_\pm$ does not depend on time, it is easy to solve Hamilton's equations

$$\pm d\omega/dx = -\partial_t K_\pm = 0 \Rightarrow \omega_\pm = \omega_0,$$
$$\pm dt_\pm/dx = \partial_\omega K_\pm \Rightarrow (t_f - t_i)_\pm = \int dx\,\partial_\omega K_\pm,$$
$$\pm d\phi_\pm/dx = -\mathcal{L}_\pm \Rightarrow (\phi_f - \phi_i)_\pm = -\int dx\,\mathcal{L}_\pm.$$

Adding both contributions we find the phase at arrival at the detector is

$$(\phi_f)_\pm + \omega t_f = (\phi_f - \phi_i)_\pm + \omega(t_f - t_i)_\pm = \int_{x_i}^{x_f} dx\,K_\pm.$$

This result was expected and could have been easily derived without use of our general formalism. The phase difference at arrival is then

$$\begin{aligned}\Delta\phi &= \int_{x_i}^{x_f} dx(K_+ - K_-)\\ &= 2[\omega\left(1 - n_0^2\right) - \omega^2 n_0\partial_\omega n_0]\int V dx + O(\beta^2)\\ &= 2\omega[1 - n_0\partial_\omega(\omega n_0)]\int V dx + O(\beta^2).\end{aligned} \tag{A11}$$

[1] Georges Sagnac, L'éther lumineux démontré par l'effet du vent relatif d'éther dans un interféromètre en rotation uniforme, Compte Rendu Acad. Sci. (Paris) **157**, 708 (1913).
[2] R. Wang, Y. Zheng, and A. Yao, Generalized Sagnac Effect, Phys. Rev. Lett. **93**, 143901 (2004).
[3] A. Ori and J. E. Avron, Generalized Sagnac-Wang-Fizeau formula, Phys. Rev. A **94**, 063837 (2016).
[4] D. M. Shupe, Thermally induced nonreciprocity in the fiber-optic interferometer, Appl. Opt. **19**, 654 (1980).
[5] W. W. Chow, J. Gea-Banacloche, L. M. Pedrotti, V. E. Sanders, W. Schleich, and M. O. Scully, The ring laser gyro, Rev. Mod. Phys. **57**, 61 (1985).
[6] V. Vali and R. W. Shorthill, Fiber ring interferometer, Appl. Opt. **15**, 1099 (1976).
[7] X. Dong, H. Y. Tam, and P. Shum, Temperature-insensitive strain sensor with polarization-maintaining photonic crystal fiber based sagnac interferometer, Appl. Phys. Lett. **90**, 151113 (2007).
[8] D.-H. Kim and J. Kang, Sagnac loop interferometer based on polarization maintaining photonic crystal fiber with reduced temperature sensitivity, Opt. Express **12**, 4490 (2004).
[9] R. Anderson, H. R. Bilger, and G. E. Stedman, Sagnac effect: A century of earth rotated interferometers, Am. J. Phys. **62**, 975 (1994).
[10] H. J. Arditty and H. C. Lefevre, Sagnac effect in fiber gyroscopes, Opt. Lett. **6**, 401 (1981).
[11] F. Hasselbach and M. Nicklaus, Sagnac experiment with electrons: Observation of the rotational phase shift of electron waves in vacuum, Phys. Rev. A **48**, 143 (1993).
[12] F. Riehle, Th. Kisters, A. Witte, J. Helmcke, and Ch. J. Bordé, Optical Ramsey Spectroscopy in a Rotating Frame: Sagnac Effect in a Matter-Wave Interferometer, Phys. Rev. Lett. **67**, 177 (1991).
[13] J. Bauchrowitz, V. Händchen, H. Vahlbruch, M. Mehmet, H. Müller-Ebhardt, T. Eberle, S. Steinlechner, and R. Schnabel, Quantum Enhancement of the Zero-Area Sagnac Interferometer Topology for Gravitational Wave Detection, Phys. Rev. Lett. **104**, 251102 (2010).
[14] T. L. Gustavson, A. Landragin, and M. A. Kasevich, Rotation sensing with a dual atom-interferometer Sagnac gyroscope, Class. Quantum Grav. **17**, 2385 (2000).
[15] S. Schiller, Feasibility of giant fiber-optic gyroscopes, Phys. Rev. A **87**, 033823 (2013).
[16] G. B. Malykin, The Sagnac effect: Correct and incorrect explanations, Phys. Usp. **43**, 1229 (2000).
[17] E. J. Post, Sagnac effect, Rev. Mod. Phys. **39**, 475 (1967).
[18] G. E. Stedman, Ring-laser tests of fundamental physics and geophysics, Rep. Prog. Phys. **60**, 615 (1997).
[19] L. N. Menegozzi and W. E. Lamb, Jr., Theory of a ring laser, Phys. Rev. A **8**, 2103 (1973).
[20] T. Shiozawa, Phenomenological and electron-theoretical study of the electrodynamics of rotating systems, Proc. IEEE **61**, 1694 (1973).
[21] V. I. Arnold, *Lectures on Partial Differential Equations* (Springer, New York, 2004).
[22] S. A. Newton, C. C. Cutler, and H. J. Shaw, Limitation of rotation sensing by scattering, Opt. Lett. **5**, 488 (1980).
[23] M. K. Balyan, Transport equations of amplitudes in the eikonal approximation of dynamical diffraction equations, J. Contemp. Phys. **48**, 46 (2012).
[24] M. H. Fizeau, Sur les hypothèses relatives à l'éther lumineux, et sur une expérience qui parait démontrer que le mouvement des corps change la vitesse avec laquelle la lumière se propage dans leur intérieur, Compte Rendu Acad. Sci. **33**, 349 (1851).
[25] M. von Laue, Die mitführung des lichtes durch bewegte körper nach dem relativitätsprinzip, Ann. Phys. (Berlin, Ger.) **328**, 989 (1907).
[26] F. John, *Partial Differential Equations* (Springer, New York, 1991).
[27] S. Levit and U. Smilansky, Ann. Phys. (NY) **108**, 165 (1977).